Thermophysical Properties of Imidazolium-Based Ionic Liquids: The Effect of Aliphatic versus Aromatic Functionality

ARTICLE *in* JOURNAL OF CHEMICAL & ENGINEERING DATA · SEPTEMBER 2014

Impact Factor: 2.04 · DOI: 10.1021/je500185r

Journal of chemical & engineering data

Article

pubs.acs.org/jced

Thermophysical Properties of Imidazolium-Based Ionic Liquids: The Effect of Aliphatic versus Aromatic Functionality

Ran Tao,[†] George Tamas,[‡] Lianjie Xue,[‡] Sindee L. Simon,*[,†] and Edward L. Quitevis*[,‡]

[†]Department of Chemical Engineering, and [‡]Department of Chemistry & Biochemistry, Texas Tech University, Lubbock, Texas 79409, United States

Supporting Information

ABSTRACT: In this work, a series of imidazolium-based ionic liquids with varying functionalities from aliphatic to aromatic groups and a fixed anion, bis[(trifluoromethane)-sulfonyl]amide, were investigated. The imidazolium cations included 1-heptyl-3-methylimidazolium, 1-(cyclohexylmethyl)-3-methylimidazolium, 1-benzyl-3-methylimidazolium, 1,3-dibenzylimidazolium, and 1-(2-naphthylmethyl)-3-methylimidazolium. Structure−property relationships were investigated regarding the substituent effects on the imidazolium cation, including *n*-alkyl versus cycloalkyl and aromatic versus aliphatic, as well as the effects of cation symmetry and larger aromatic polycyclic functionalities. Thermophysical properties investigated include density, thermal transition temperatures, and decomposition temperatures. The densities of the ionic liquids are governed by the substituents on the cation: *n*-alkyl < cycloalkyl < aromatic. The group contribution method is applicable for the density estimation of ionic liquids, and the volume parameters for cyclohexyl, phenyl, and naphthyl groups are reported. The glass transition temperature (T_g) follows the same systematic trend due to substituent flexibility: *n*-alkyl < cycloalkyl < aromatic. Thermal stability as measured by dynamic thermogravimetric analysis (TGA) is not strongly affected by the substituents on the imidazolium ring; however, slight differences are observed with the higher T_g ionic liquids having lower decomposition temperatures for this series of ionic liquids. On the other hand, the cyclohexylmethyl-substituted ionic liquid exhibits a higher activation energy for degradation than the other ionic liquids based on isothermal TGA, and all ionic liquids studied show significant weight loss at 300 °C indicating that appreciable decomposition can occur at temperatures substantially lower than the onset temperature observed in dynamic TGA scans.

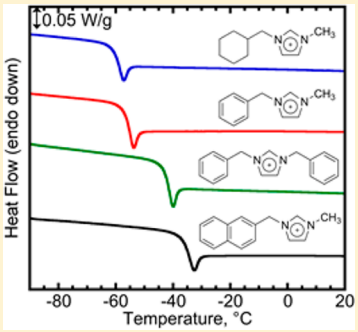

1. INTRODUCTION

As a material class, ionic liquids are organic salts composed entirely of ions. They are usually liquid at room temperature with melting points at or below 373 K. The most attractive features of ionic liquids are their negligible vapor pressure, as well as the ability to tune their physicochemical properties by varying the ion structure; the latter has led to their being known as "designer" solvents.[1] These two key features along with other properties, such as good thermal stability, high ionic conductivity, good solvation ability, and a wide electrochemical window, make ionic liquids excellent candidates for a wide range of uses, including uses as solvents or catalysts for reactions,[2] lubricants,[3] heat transfer fluids,[4] electrolytes,[5] and media for gas absorption[6] and for liquid separation processes.[7]

Thermophysical properties are of utmost importance for the design of new ionic liquids to meet specific requirements; for example, the glass transition, melting, and decomposition temperatures determine the liquid operating temperature range. Since the variation of ion pairs gives rise to a great number of ionic liquids with a wide variety of properties, an understanding of structure−property relationships is helpful. Of all ionic liquids, the 1-alkyl-3-methylimidazolium- and the 1,3-dialkylimidazolium-based materials are the most studied in the literature, and several general trends of thermophysical properties for these ionic liquids have been observed. For example, as the substituted alkyl chain length on the imidazolium cation increases, the density of ionic liquids decreases,[8−12] glass transition temperature (T_g) increases,[9] and thermal stability remains nearly unchanged.[11−13]

In this work, we are interested in investigating the effects of aromaticity and substituent flexibility on the thermophysical properties of ionic liquids. Previously, Nishikawa and co-workers[14] studied the effects of cycloalkyl and *n*-alkyl substituents on physicochemical properties of imidazolium ionic liquids and their associated reorientational dynamics using ^{13}C NMR spectroscopy. In a subsequent report,[15] they examined the effects of the alkyl linker length for the cyclic and aromatic substituents. Several other authors[16−18] reported the physicochemical properties of ionic liquids based on phenyl-containing imidazolium cations. However, none of these studies gives a clear description of the correlation between aromaticity and the thermophysical properties of the corresponding ionic liquids, and that is an aim of the current work.

For this purpose, a series of ionic liquids consisting of a fixed bis[(trifluoromethane)sulfonyl]amide anion ($[NTf_2]^-$) and a 1-

Received: February 23, 2014
Accepted: July 16, 2014
Published: July 30, 2014

Table 1. Structures of Imidazolium-Based Cations Varying from Aliphatic to Aromatic Functionalities Investigated in this Study

cation	cation structure	abbreviation	formula	CAS no. for ILs
1-heptyl-3-methylimidazolium	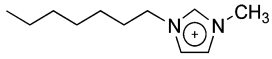	$[C_7C_1im]^+$	$C_{11}H_{21}N_2^+$	425382-14-5
1-(cyclohexylmethyl)-3-methylimidazolium	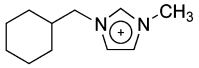	$[CyhmC_1im]^+$	$C_{11}H_{19}N_2^+$	1309854-95-2
1-benzyl-3-methylimidazolium	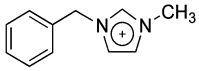	$[BnzC_1im]^+$	$C_{11}H_{13}N_2^+$	433337-24-7
1,3-dibenzylimidazolium	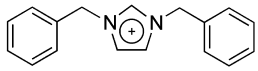	$[(Bnz)_2im]^+$	$C_{17}H_{17}N_2^+$	958869-88-0
1-(2-naphthylmethyl)-3-methylimidazolium	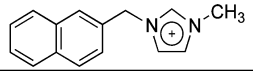	$[NapmC_1im]^+$	$C_{15}H_{15}N_2^+$	1312342-01-0

R-3-methylimidazolium cation functionalized by various R groups were synthesized, with R = heptyl (C_7), cyclohexylmethyl (Cyhm), benzyl (Bnz), and 2-naphthylmethyl (Napm). Of these, the naphthyl-derivatized imidazolium ionic liquid 1-(2-naphthylmethyl)-3-methylimidazolium bis[(trifluoromethane)sulfonyl]amide is a new ionic liquid whose properties have not, to the best of our knowledge, been previously reported, although a patent on its preparation exists.[19] This series of ionic liquids allows us to examine the effect of substituent structure, including *n*-alkyl versus cycloalkyl, aromatic versus aliphatic, and the effect of larger aromatic polycyclic substituents, on their thermophysical properties (density, thermal transition temperatures and decomposition temperatures). Additionally, a symmetric cation-based ionic liquid, 1,3-dibenzylimidazolium bis[(trifluoromethane)-sulfonyl]amide, was prepared by incorporating two rigid benzyl groups on the imidazolium ring. By a comparison of the properties of this ionic liquid with the properties of the monobenzyl-substituted counterpart, the influence of cation symmetry was studied as well. The structures and abbreviations, as well as the CAS numbers, of all imidazolium-based cations investigated in this study are summarized in Table 1. For convenience, abbreviations based on the functional groups on the imidazolium ring will be used in the following sections.

2. EXPERIMENTAL SECTION

2.1. Materials and Synthesis. All reagents and solvents were purchased from commercial sources (Sigma-Aldrich, Acros Organics, 3M) and were used as received. All reactions were run under nitrogen atmosphere and using oven-dried glassware. The synthesis of $[C_7C_1im][NTf_2]$ and $[BnzC_1im][NTf_2]$ has been reported previously.[10] The synthesis of other imidazolium-based ionic liquids used in this study is described in the Supporting Information, along with the ^{1}H NMR, ^{13}C NMR, and ^{19}F NMR spectroscopy data for the new ionic liquid $[NapmC_1][NTf_2]$. After synthesis, the samples were kept in tightly sealed vials and stored in an argon-filled glovebox or desiccators. Prior to any measurements, the ionic liquids were vacuum-dried at 50 °C for at least 24 h, and their water contents, as determined by Karl Fischer titration using a Mettler-Toledo DL36 coulometer, ranged from 20 ppm to 125 ppm. When in use, the ionic liquids were constantly under an argon atmosphere or kept in a closed system to prevent adventitious water absorption.

2.2. Density Measurements. Densities of the ionic liquids were measured as a function of temperature using an Anton Paar Density Measuring System (DMA 602 density measuring cell and DMA 60 density meter) equipped with temperature control from a water bath cooler/circulator. The calibration was done by performing measurements for air and deionized water. The calibration was verified by measuring the density of acetone; based on this measurement, the accuracy is considered to be better than ± 0.001 g·cm^{-3}. Samples were transferred to a gastight syringe inside an argon-filled glovebox and introduced into the density meter in a very short period of time to minimize adventitious water absorption.

2.3. Differential Scanning Calorimetry. Calorimetric measurements were performed under nitrogen atmosphere using a Mettler-Toledo differential scanning calorimeter DSC1 equipped with a liquid nitrogen cooling system. Samples were sealed in PerkinElmer 20 μL hermetic aluminum pans in the argon-filled glovebox to minimize moisture uptake. The DSC temperature was calibrated on heating at 10 K/min using octane (T_m = −57 °C) and mercury (T_m = −38.8 °C). The heat flow calibration was performed using octane (ΔH_f = 180.0 J/g). The calibrations were checked periodically during heating using the above calibration standards during calorimetric studies.

Measurements of the limiting fictive temperature, T_f', were performed from −120 °C to 40 °C after cooling from 40 °C to −120 °C at 10 K/min. We refer to T_f' as the calorimetric T_g in the results section since T_f' measured on heating after cooling at a given rate q approximates, within 1 K, T_g measured on cooling at the same rate q.[20] T_f' was determined by integrating the heat capacity curve based on heating scans, a procedure proposed by Moynihan et al.:[21]

$$\int_{T_f'}^{T\gg T_g} (C_{pl} - C_{pg})\,dT = \int_{T\ll T_g}^{T\gg T_g} (C_p - C_{pg})\,dT \quad (1)$$

where C_{pl} and C_{pg} are the liquid and glass heat capacities, and C_p is the apparent heat capacity of the sample measured by DSC, all three of which are functions of temperature. The standard deviation for T_g (T_f') is 0.1 K based on multiple runs on the same sample. The corresponding change in heat capacity at T_g ($\Delta C_p = C_{pl} - C_{pg}$) has a standard deviation of less than 0.01 J·K^{-1}·g^{-1}. For samples that showed some crystallinity upon long-term storage, the melting temperature (T_m) was determined as the onset of the endothermic melting peak, and its enthalpy change (ΔH_m) was calculated from the peak area. On the basis of multiple runs on different crystalline samples, T_m values are considered to be within ± 0.6 K and values of ΔH_m are ± 1.3 J·g^{-1}.

2.4. Thermogravimetric Analysis. The decomposition temperatures of the ionic liquids were measured using a

Mettler-Toledo TGA/SDTA851e thermogravimetric analyzer under nitrogen atmosphere. The mass of TGA samples varied from 20 mg to 30 mg. All samples were placed in 70 μL alumina pans for the measurements. Multiple runs were performed on each ionic liquid to verify reproducibility. The thermal stability of the ionic liquids was determined using both dynamic and isothermal methods. For the dynamic method, samples were heated from 25 °C to 600 °C at a heating rate of 10 K/min. The decomposition temperatures are reported in terms of T_{start} (the temperature at which the decomposition of the sample starts), $T_{10\%}$ (the temperature at which a mass loss of 10% is reached), T_{peak} (the peak temperature of the time derivative of the mass loss curve, d(mass)/dt), and T_{onset} (the intersection of the zero mass loss baseline and the tangent line through T_{peak}). The standard deviations of decomposition temperatures reported are considered to be within 3, 1, 2, and 5 °C for T_{start}, $T_{10\%}$, T_{peak}, and T_{onset}, respectively. For the isothermal method, weight loss was measured at 300, 330, and 360 °C for 10, 4, and 2 h, respectively.

3. RESULTS AND DISCUSSION

3.1. Densities. The densities of the ionic liquids studied are shown as a function of temperature in Figure 1, including

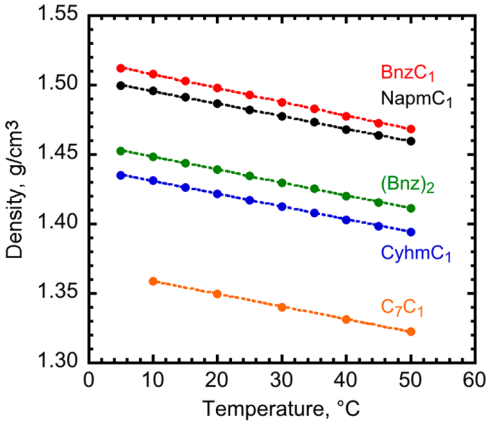

Figure 1. Density as a function of temperature for $[C_7C_1im][NTf_2]$,[9] $[CyhmC_1im][NTf_2]$, $[BnzC_1im][NTf_2]$, $[(Bnz)_2im][NTf_2]$, and $[NapC_1im][NTf_2]$ samples. See Table 2 for the density values. Dashed lines are linear fits of the equation $\rho = \rho_0 - aT$ to the data, with fitting parameters given in Table 3.

density for the *n*-alkyl substituted $[C_7C_1im][NTf_2]$ measured by Zheng et al.[9] The densities decrease linearly with increasing temperature in the range of 5 °C to 50 °C. The density values are tabulated in Table 2, and the values of linear fit parameters are listed in Table 3 along with the water content for each sample. The densities increase in the following order: C_7C_1 < $CyhmC_1$ < $(Bnz)_2$ < $NapmC_1$ < $BnzC_1$. The presence of the cycloalkyl group in place of the *n*-alkyl group with the same number of carbons leads to an increase in density, and aromatic substituents on the imidazolium cation further increase the density compared to its aliphatic analogues (*n*-alkyl or cycloalkyl); increasing the number of aromatic rings from phenyl to naphthyl results in a decrease in density; and the symmetric dibenzyl functionality gives a lower density for the ionic liquid compared to the monobenzyl counterpart. The density trend can be roughly related to the C/H ratio in the substituents, with density increasing with increasing C/H ratio from *n*-alkyl, cycloalkyl, to aromatic functionalities.

A similar temperature dependence of densities is observed for all imidazolium $[NTf_2]^-$-based ionic liquids independent of aliphatic or aromatic functionality. In fact, the slope $\alpha = d\rho/dT$ varies from 9.0 to $9.9 \cdot 10^{-4}$ g·cm^{-3}·K^{-1}, as shown in Table 3, and falls within the range of literature values (8.8 to $10.6 \cdot 10^{-4}$ g·cm^{-3}·K^{-1}) for 1-alkyl-3-methylimidazolium and 1,3-dialkylimidazolium ionic liquids containing the same $[NTf_2]^-$ anion.[9,12]

The molar volumes of the ionic liquids at 25 °C calculated from the molar mass and density are tabulated in Table 4. Also shown in the table are values of the theoretical molar van der Waals volume (vdW) and the volume (the difference between the experimental molar volume and the molar van der Waals volume) for each sample. The theoretical molar vdW volume follows the order $BnzC_1$ < $CyhmC_1$ < $NapmC_1$ < C_7C_1 < $(Bnz)_2$, which is in good agreement with the molar volume obtained from the density measurement: $BnzC_1$ < $CyhmC_1$ < C_7C_1 < $NapmC_1$ < $(Bnz)_2$, except for the *n*-alkyl substituted imidazolium ionic liquid C_7C_1. C_7C_1 is considered a special case among these structurally similar cations with its higher free volume attributed to the decreased packing efficiency of the long alkyl chain.

The group contribution method has been successfully applied to ionic liquids for the estimation of the density by Ye and Shreeve[22] following the work on ionic solids by Jenkins et al.[23] We applied the group contribution method using Ye and Shreeve's volume parameters tabulated for the imidazolium cation, anion, and alkyl groups to our previous study[9] of symmetric and asymmetric imidazolium based ionic liquids having various alkyl chain lengths; we found that densities were predicted within 0.005 g·cm^{-3} independent of cation symmetry, as shown in Table 5 (entries 1 to 8). Consequently, we use Ye and Shreeve's volume parameters to fit the ionic liquids studied in this work, as well as to fit data from Mandai et al.,[15] and in fitting these data, we obtain the volume parameters for the cyclic and aromatic groups. The parameters are listed in Table 6, and predicted densities for our ionic liquids are presented in Table 5 (entries 9 to 12); predictions are within 0.008 g·cm^{-3} of experimental values. Also shown in Table 5 is the

Table 2. Densities for Ionic Liquids as a Function of Temperature[a]

	ρ (T, °C), g·cm^{-3}									
ionic liquid	T/°C = 5	T/°C = 10	T/°C = 15	T/°C = 20	T/°C = 25	T/°C = 30	T/°C = 35	T/°C = 40	T/°C = 45	T/°C = 50
$[C_7C_1im][NTf_2]$[b]		1.359		1.350		1.340		1.331		1.322
$[CyhmC_1im][NTf_2]$	1.435	1.431	1.426	1.422	1.417	1.412	1.408	1.403	1.398	1.394
$[BnzC_1im][NTf_2]$	1.512	1.508	1.503	1.498	1.493	1.488	1.483	1.478	1.473	1.468
$[(Bnz)_2im][NTf_2]$	1.452	1.448	1.444	1.439	1.434	1.430	1.425	1.420	1.415	1.411
$[NapmC_1im][NTf_2]$	1.500	1.496	1.491	1.486	1.482	1.477	1.473	1.468	1.464	1.459

[a]Standard uncertainties u are $u(T)$ = 0.02 °C and $u(\rho)$ = 0.001 g·cm^{-3}. [b]Density data for $[C_7C_1im][NTf_2]$ are from Zheng et al.[9]

dx.doi.org/10.1021/je500185r | J. Chem. Eng. Data 2014, 59, 2717−2724

Table 3. Density Parameters[a] and Water Content for Ionic Liquids

ionic liquid	ρ_0, g·cm^{-3}	a, 10^{-4} g·cm^{-3}·°C^{-1}	water content[b], μg·g^{-1}
$[C_7C_1im][NTf_2]$[c]	1.368 ± 0.001	9.13 ± 0.22	21.9
$[CyhmC_1im][NTf_2]$	1.440 ± 0.001	9.18 ± 0.18	23.4
$[BnzC_1im][NTf_2]$	1.517 ± 0.001	9.88 ± 0.18	107.2
$[(Bnz)_2im][NTf_2]$	1.458 ± 0.001	9.32 ± 0.18	27.5
$[NapmC_1im][NTf_2]$	1.504 ± 0.001	9.02 ± 0.19	125.0

[a]Parameters correspond to the linear least-squares fit of the equation $\rho = \rho_0 - aT$ to the density vs temperature data in Figure 1 in the temperature range of 5 °C to 50 °C. [b]Water contents were determined by Karl Fischer titration. [c]Density data for $[C_7C_1im][NTf_2]$ are from Zheng et al.[9]

Table 4. Volumetric Properties of Ionic Liquids at 25 °C

ionic liquid	molar mass g·mol^{-1}	density[a] g·cm^{-3}	molar volume cm^3·mol^{-1}	molar vdW volume[b] cm^3·mol^{-1}	free volume[c] cm^3·mol^{-1}
$[C_7C_1im][NTf_2]$	461.4	1.345[d]	343.0	232.9	110.1
$[CyhmC_1im][NTf_2]$	459.4	1.417	324.2	224.5	99.7
$[BnzC_1im][NTf_2]$	453.4	1.493	303.7	217.2	86.5
$[(Bnz)_2im][NTf_2]$	529.5	1.434	369.2	267.6	101.6
$[NapmC_1im][NTf_2]$	503.4	1.482	339.7	247.8	91.9

[a]Standard uncertainty u for density is $u(\rho)$ = 0.001 g·cm^{-3}. [b]Values of molar van der Waals volume (vdW) were calculated using the quantum chemistry program Spartan (Wave function, Inc.). [c]Free volume = molar volume − molar vdW volume. [d]Density data for $[C_7C_1im][NTf_2]$ are interpolated from Zheng et al.[9]

Table 5. Prediction of Densities of Ionic Liquids at 25 °C

		density, g·cm^{-3}	
entry	ionic liquid	experiment[a]	prediction
1	$[C_3C_1im][NTf_2]$	1.475[b]	1.470
2	$[C_2C_2im][NTf_2]$	1.473[b]	1.470
3	$[C_5C_1im][NTf_2]$	1.404[b]	1.400
4	$[C_3C_3im][NTf_2]$	1.400[b]	1.400
5	$[C_7C_1im][NTf_2]$	1.345[b]	1.344
6	$[C_4C_4im][NTf_2]$	1.342[b]	1.344
7	$[C_9C_1im][NTf_2]$	1.298[b]	1.298
8	$[C_5C_5im][NTf_2]$	1.295[b]	1.298
9	$[CyhmC_1im][NTf_2]$	1.417	1.415
10	$[BnzC_1im][NTf_2]$	1.493	1.488
11	$[(Bnz)_2im][NTf_2]$	1.434	1.441
12	$[NapmC_1im][NTf_2]$	1.482	1.482
13	$[CyheC_1im][NTf_2]$	1.386[c]	1.387
14	$[CyhpC_1im][NTf_2]$	1.358[c]	1.361
15	$[BnzmC_1im][NTf_2]$	1.456[c]	1.454
16	$[BnzeC_1im][NTf_2]$	1.434[c]	1.423

[a]Standard uncertainty u for experimental density is $u(\rho)$ = 0.001 g·cm^{-3} for our data and data from ref 9 (entries 1 to 12). [b]Values interpolated from Zheng et al.;[9] abbreviations follow nomenclature described in Zheng et al. [c]Values from Mandai et al.;[15] abbreviations follow our nomenclature as described in the text.

Table 6. Volume Parameters of Groups and Fragments for Ionic Liquids

	volume (Å^3)		
species or groups	ionic liquids	ionic solids	organic liquids
1,3-dimethylimidazolium	154[a]	125[a]	
NTf_2^-	248[a]	238[a]	
CH_2 (acyclic)	28[a]	24[a]	26.7 to 27.6[b]
CH_3	35[a]	30[a]	
cyclohexyl	144	132[a]	128.2 to 131.0[b]
phenyl	111		97.3 to 102.6[b]
naphthyl	169		

[a]Values from Ye and Shreeve.[22] [b]Range of values in refs 24 to 26.

comparison between experiment and predicted densities for Mandai's ionic liquids (entries 13 to 16), which contain cyclic and aromatic substituents with one or two additional methylene groups on the imidazolium cation, that is, cyclohexylethyl (Cyhe), cyclohexylpropyl (Cyhp), benzylmethyl (Bnzm), and benzylethyl (Bnze) following our nomenclature.

The volume contribution of a methylene group in ionic liquids was previously found to be larger than that in ionic solids and in organic liquids;[22] the comparison is shown in Table 6. We similarly find this to be the case for cyclohexyl and phenyl groups, as shown in the table. We attribute the larger volumes to the hydrophobic effect, that is, to the exclusion of hydrocarbon from regions of high-charge density. This finding is important in that it impacts our understanding of the nature of the hydrocarbon regions in ionic liquids; specifically, the finding indicates that the properties of the hydrocarbon regions in ionic liquids will not be the same as in an equivalent organic liquid.

3.2. Glass-Transition and Melting Temperatures. The normalized DSC heat flow responses measured on heating at 10 K/min after cooling at 10 K/min for the ionic liquids investigated are shown in Figure 2. A characteristic step change in heat capacity corresponding to the glass transition is identified for all samples. No other transition behavior such as cold crystallization or melting is observed on heating. The glass transition temperatures ($T_g \approx T_f'$) and their associated change in heat capacity ΔC_p for each sample are presented in Table 7, along with values for the *n*-alkyl ionic liquid $[C_7C_1][NTf_2]$ measured by Zheng et al.[9] The T_g of the series of imidazolium-based ionic liquids with different substituents on the cation increases in the order C_7C_1 < $CyhmC_1$ < $BnzC_1$ < $(Bnz)_2$ < $NapmC_1$. This trend gives a clear illustration of how chain flexibility influences T_g: the more rigid the substituent is, the higher is the T_g of the ionic liquid. For the ionic liquids containing the same number of carbons, the phenyl ring substituted cation has the highest T_g, second is the cycloalkyl cation, whereas the *n*-alkyl substituted cation shows the lowest T_g; that is, $BnzC_1$ > $CyhmC_1$ > C_7C_1. For the aromatic ring substituted cations, the ionic liquid with the larger polycyclic substituent exhibits higher T_g than that with a single ring, that

dx.doi.org/10.1021/je500185r | J. Chem. Eng. Data 2014, 59, 2717−2724

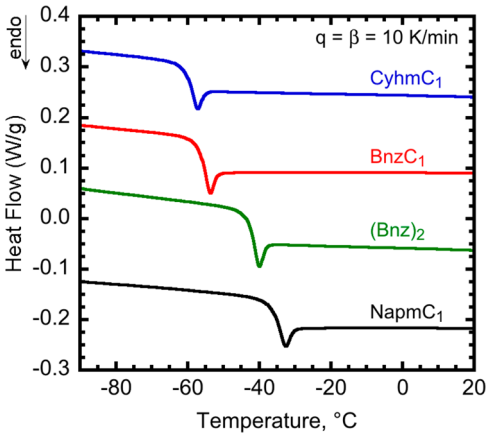

Figure 2. DSC heating scans at 10 K/min after cooling at 10 K/min for $[CyhmC_1im][NTf_2]$, $[BnzC_1im][NTf_2]$, $[(Bnz)_2im][NTf_2]$, and $[NapmC_1im][NTf_2]$ ionic liquids. DSC scans are offset for clarity. See Table 7 for thermal parameters.

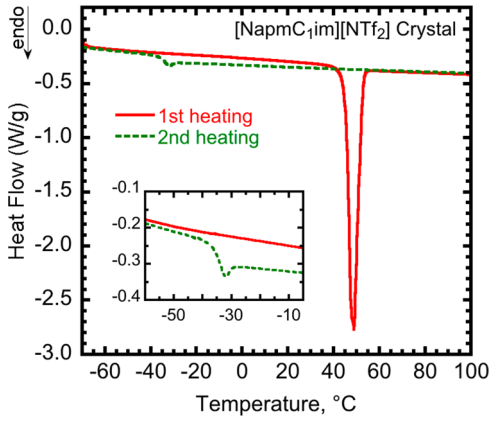

Figure 3. DSC heating scans at 10 K/min after cooling at 10 K/min for crystalline $[NapmC_1im][NTf_2]$ ionic liquid sample. Inset figure shows enlarged view of heat flow responses in the glass transition region. See Table 7 for thermal parameters.

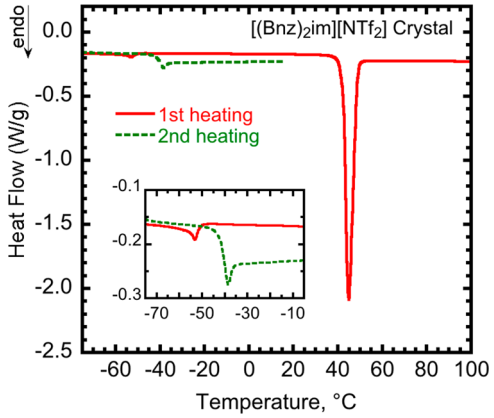

Figure 4. DSC heating scans at 10 K/min after cooling at 10 K/min for crystalline $[(Bnz)_2im][NTf_2]$ ionic liquid sample. Inset figure shows enlarged view of heat flow responses in the glass transition region. See Table 7 for thermal parameters.

is, $NapmC_1$ > $BnzC_1$. The symmetric dibenzyl salt shows a higher T_g than the asymmetric salt with only one benzyl group, $(Bnz)_2$ > $BnzC_1$. The T_g trend observed for ionic liquids is similar to the structure–T_g relationships observed for polymers, in which chain and substituent flexibility are the controlling factors.[27,28]

$[NapmC_1im][NTf_2]$ and $[(Bnz)_2im][NTf_2]$ samples were found to form crystals over the course of the study (two months). Figure 3 shows the DSC normalized heat flow response for the crystalline $[NapmC_1im][NTf_2]$ sample. A sharp endothermic peak at T_m = 45.4 °C corresponding to a melting transition with an enthalpy ΔH_m = 67.7 J/g is observed on the first heating scan, whereas on the second heating scan (see Figure 3 inset) only the glass transition is present. Figure 4 shows the corresponding DSC heating scans for a crystalline $[(Bnz)_2im][NTf_2]$ sample with a melting transition at T_m = 41.7 °C. An unusual endothermic peak is observed on the first heating scan (see Figure 4 inset), which most likely corresponds to a solid–solid transition in the glassy state. The melting parameters for both crystalline samples are presented in Table 7.

For both $[(Bnz)_2im][NTf_2]$ and $[NapmC_1im][NTf_2]$ crystalline samples, no exothermic crystallization peak was observed upon cooling (not shown), indicating that the time scale of crystallization process is longer than the duration of the experimental time window. This, together with the fact that the liquid samples solidified at room temperature only after long times, indicates that neither $[NapmC_1im][NTf_2]$ nor $[(Bnz)_2im][NTf_2]$ ionic liquids are easily crystallized. However, relatively speaking, $[(Bnz)_2im][NTf_2]$ is observed to form crystals much easier compared to $[NapmC_1im][NTf_2]$, which is

Table 7. Thermal Properties of Ionic Liquids[a,b]

ionic liquid	T_g / °C	ΔC_p / J·K^{-1}·g^{-1}	T_m / °C	ΔH_m / J·g^{-1}	T_{start} / °C	$T_{10\%}$ / °C	T_{peak} / °C	T_{onset} / °C	E_a / kJ·mol^{-1}
$[C_7C_1im][NTf_2]$	−85.3[c]	0.36[d]			377	426	464	437	111
$[CyhmC_1im][NTf_2]$	−62.4	0.36			376	413	470	429	156
$[BnzC_1im][NTf_2]$	−58.3	0.43			372	402	464	421	121
$[(Bnz)_2im][NTf_2]$	−44.7	0.42	41.7[d]	44.6	367	391	453	410	149
$[NapmC_1im][NTf_2]$	−38.4	0.37	45.4[d]	67.7	357	392	460	406	136

[a] T_g, glass transition temperature; ΔC_p, heat capacity change at T_g; T_m, melting temperature; ΔH_m, enthalpy of melting; T_{start}, the start temperature of decomposition in dynamic TGA; $T_{10\%}$, temperature at 10% mass loss; T_{peak}, peak temperature of d(mass)/dt curves; T_{onset}, the intersection of the zero mass loss baseline and the tangent line through T_{peak}; E_a, apparent activation energy for thermal degradation. [b] Standard uncertainties u are $u(T_g)$ = 0.1 °C, $u(\Delta C_p)$ = 0.01 J·K^{-1}·g^{-1}, $u(T_m)$ = 0.6 °C, $u(\Delta H_m)$ = 1.3 J·g^{-1}, $u(T_{start})$ = 3 °C, $u(T_{10\%})$ = 1 °C, $u(T_{peak})$ = 2 °C, $u(T_{onset})$ = 5 °C, $u(E_a)$ = 6 kJ·mol^{-1} for $[BnzC_1im][NTf_2]$ and [(Bnz)2im][NTf_2], and $u(E_a)$ = 2 kJ·mol^{-1} for the other ionic liquids. [c] Reference 9. [d] T_m measurements of $[(Bnz)_2im][NTf_2]$ and $[NapmC_1im][NTf_2]$ were not taken in the same scan as T_g given that the ionic liquid samples had to be stored at room temperature for a period of time to allow crystallization; T_m was obtained from the first heating scan on the crystalline samples.

dx.doi.org/10.1021/je500185r | J. Chem. Eng. Data 2014, 59, 2717–2724

not surprising because of the symmetric nature of the dibenzyl cation. In addition, values of the T_m/T_g ratio for both crystalline ionic liquids are found to be around 1.4, slightly lower than the nominal value of 1.5 ($T_g/T_m \approx 2/3$) for glass-formers.[29] Similar values of T_m to T_g ratio were reported by Angell and co-workers[30] on several alkyl ammonium-based chelated orthoborate ionic liquids with T_g and T_m obtained on separate scans with different thermal histories. The authors suggested that the difficult-to-crystallize samples will have lower T_m/T_g ratios and that the well-known "2/3 Kauzmann–Beaman rule"[29] is only applicable to substances that may readily form glasses and crystals.[30]

3.3. Decomposition Temperatures. The dynamic TGA curves of the ionic liquids at a heating rate of 10 K/min are shown in Figure 5 with the inset showing the time derivative of

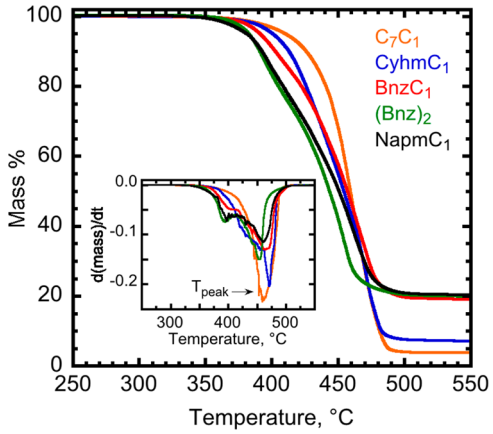

Figure 5. Dynamic TGA curves (heating rate = 10 K/min) for the imidazolium-based ionic liquids studied. Inset figure shows the normalized rate of the mass loss (min^{-1}) as a function of temperature.

the mass loss curve (d(mass)/dt), both as a function of temperature. Values of T_{start}, $T_{10\%}$, T_{peak}, and T_{onset} for each sample are listed in Table 7. Although dynamic TGA experiments overestimate thermal stability,[31−36] the decomposition temperatures are often useful as comparative indicators of the short-term thermal stability of the ionic liquids. As can be seen from the values of T_{start} and T_{onset} in Table 7, the short-term stability of the studied liquids decreases in the order C_7C_1 > $CyhmC_1$ > $BnzC_1$ > $(Bnz)_2$ > $NapmC_1$. This trend seems to be in contrast to the T_g trend: the lower is the T_g, the more stable is the ionic liquid. Furthermore, the ionic liquids with aliphatic substituted cations show an overall better stability than the aromatic analogues, in agreement with the work of Erdmenger et al.[17] in which they found that ionic liquids with the $[BnzC_1im]^+$ cation exhibited lower stabilities than their n-alkyl analogues with the $[BF_4]^-$ anion. Additionally, the benzyl/naphthylmethyl-containing ionic liquids exhibit similar weight loss at the end of the scan, higher than the ionic liquids with only aliphatic moieties exhibit. The ionic liquid containing the n-alkyl cation $[C_7C_1im]^+$ is most stable with the highest onset decomposition temperature of 436 °C. However, it shows a greater mass loss as seen by the dynamic TGA curve (Figure 5), as well as observed in the d(mass)/dt curve (inset of Figure 5) where a sharp downward peak is present.

Figure 6 shows the isothermal TGA curves of the ionic liquids measured at 300 °C as a function of time. Aromatic-containing ionic liquids ($BnzC_1$, $(Bnz)_2$, and $NapmC_1$) show significant weight loss, that is, up to nearly 50% on holding for

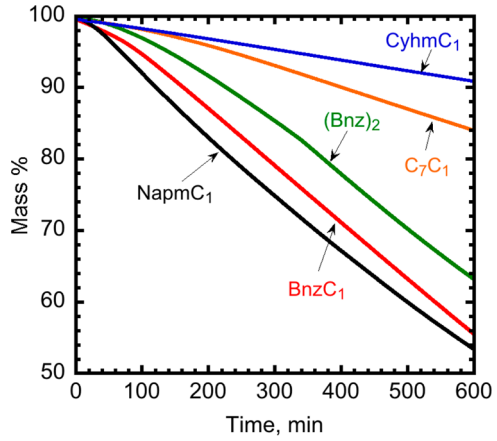

Figure 6. Isothermal TGA at 300 °C for the imidazolium-based ionic liquids studied.

10 h at 300 °C; whereas the aliphatic $CyhmC_1$ and C_7C_1 exhibit better long-term thermal stability with less than 16% weight loss. The isothermal test temperature is at least 100 °C lower than the T_{onset} measured in the dynamic scans. This observation is not surprising since weight loss is a function of time and temperature, such that fast heating gives significant weight loss only at temperatures higher than at the temperature where the actual degradation starts to take place. Other reports have similarly pointed out that ionic liquids exhibit appreciable decomposition at temperatures substantially lower than the onset temperature reported from dynamic TGA scans.[31−36]

The kinetics of decomposition can be analyzed using isothermal decomposition data obtained at various temperatures.[35,36] The rate of mass loss can be expressed as

$$\frac{dm}{dt} = kf(m) \tag{2}$$

where m is the normalized mass (mass %) and k is the rate constant, which is assumed to follow the Arrhenius equation:

$$k = A \exp\left(-\frac{E_a}{RT}\right) \tag{3}$$

where E_a is the apparent activation energy and A is the pre-exponential factor. No assumption for the form of the rate expression $f(m)$ in eq 2 is needed to obtain the apparent activation energy E_a, using the time–temperature superposition method.[37] Combining the above two equations, rearranging, and integrating yields

$$\ln \int_0^m \frac{dm}{f(m)} = \ln A + \ln t - \frac{E_a}{RT} \tag{4}$$

The left-hand side of eq 4 is a constant at a given mass %, and we can define the time–temperature horizontal shift factor, a_T, as the difference in time in natural logarithmic scale between two curves at a given mass %:

$$\ln a_T = \ln t(T_{ref}) - \ln t(T) = -\frac{E_a}{R}\left(\frac{1}{T} - \frac{1}{T_{ref}}\right) \tag{5}$$

We plot mass (%) as a function of ln t, as shown in the left panel of Figure 7a for $NapmC_1$ and apply the superposition procedure to produce a reduced curve at T_{ref} = 300 °C, as shown in the right panel of Figure 7a for all the ionic liquids. The apparent activation energy for decomposition is then

dx.doi.org/10.1021/je500185r | J. Chem. Eng. Data 2014, 59, 2717−2724

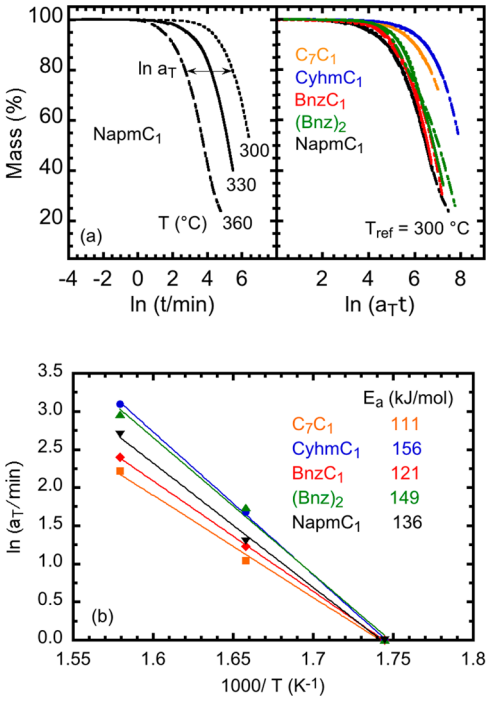

Figure 7. (a) Mass (%) versus ln t from isothermal TGA scans for $NapmC_1$ ionic liquid (left panel), and versus ln ($a_T t$) after application of horizontal shifts to T_{ref} = 300 °C for all ionic liquids studied. (b) Natural logarithm of the shift factor (a_T) as a function of 1000/T, with the apparent activation energy for decomposition indicated. View in color for best clarity.

obtained directly from the slope of the Arrhenius plot, where the shift factors are plotted logarithmically versus reciprocal temperature,[37] as shown in Figure 7b for all the ionic liquids. Activation energies range from 111 kJ·mol^{-1} for the heptyl C_7C_1 derivative to 156 kJ·mol^{-1} for the cyclohexylmethyl-substituted ionic liquid $CyhmC_1$; the high activation energy of the latter explains why $CyhmC_1$ is the most stable ionic liquid at 300 °C (Figure 6) but not at the higher temperatures accessed in the dynamic scans (Figure 5). The standard error of estimate is 2 kJ·mol^{-1} except for the $BnzC_1$ and $(Bnz)_2$ ionic liquids where the error is 6 kJ·mol^{-1}; the error was determined by performing the isoconversion method at every mass % to calculate E_a as a function of weight loss, and the higher error for the benzyl-substituted liquids arises from their poorer reduction which can be seen in the right panel of Figure 7a and which reflects a nonconstant E_a. The values of E_a for this series of ionic liquids are also listed in Table 7 along with other thermal properties.

As is well-known, the thermal stability of ionic liquids does not strongly depend on the cation structure.[11−13] Since our ionic liquids differ only in the substituents on the imidazolium ring of the cation, only small differences in the decomposition temperatures for the studied ionic liquids are observed from the dynamic TGA results, for example, less than 30 °C difference in T_{onset}. However, at 300 °C, differences are more apparent with weight loss in 10 h ranging from less than 10 % to nearly 50 %. Obviously, the mechanism of decomposition is important. In most cases, an S_N1 decomposition mechanism is proposed for benzyl-substituted imidazolium ionic liquids.[17,35,38] However, as TGA is the only technique used for degradation characterization, the specific decomposition mechanism is beyond the scope of the present paper.

4. CONCLUSIONS

The thermophysical properties of a series of imidazolium-based ionic liquids with varying functionalities from aliphatic to aromatic were investigated. A new naphthalene-derivatized imidazolium ionic liquid $[NapmC_1im][NTf_2]$ was synthesized. Structure−property relationships were investigated regarding the effect of substituents on the imidazolium cation, including *n*-alkyl versus cycloalkyl, aromatic versus aliphatic, and the effects of cation symmetry and larger aromatic polycyclic functionalities. Densities decrease linearly with increasing temperature for all samples with the same temperature dependence, indicating a similar thermal expansion coefficient regardless of substituent structure. The density follows the order C_7C_1 < $CyhmC_1$ < $(Bnz)_2$ < $NapmC_1$ < $BnzC_1$. This trend is well explained in terms of the theoretical molar van de Waals volume, and the density values are in an excellent agreement with the values predicted using the group contribution method with volume parameters for cyclohexyl, phenyl, and naphthyl groups reported. The T_g follows the systematic trend expected according to the variation in substituent flexibility. The aromatic substituted cations show higher T_g values than the aliphatic analogues, and the larger polycyclic substituents exhibit the highest T_g. For the cations having the same number of carbons, the T_g trend is observed to be *n*-alkyl < cycloalkyl < aromatic. Finally, thermal stability is not strongly dependent on different substituents on the imidazolium cation for dynamic scans; however, slight differences are observed with the higher T_g ionic liquids showing lower decomposition temperatures. In contrast, the isothermal TGA scans show weight loss at 300 °C in 10 h ranging from less than 10 % to nearly 50 %, indicating appreciable differences and that decomposition can occur at temperatures substantially lower than the onset temperature observed in dynamic TGA scans. The apparent activation energies for decomposition were found to range from 111 kJ·mol^{-1} to 156 kJ·mol^{-1} with the cyclohexyl-substituted ionic liquid having the highest activation energy and the *n*-alkyl substituted ionic liquid showing the lowest.

■ ASSOCIATED CONTENT

Supporting Information

Experimental procedure for synthesizing $[CyhmC_1im][NTf_2]$, $[(Bnz)_2im][NTf_2]$, and $[NapmC_1im][NTf_2]$. The ^{1}H NMR, ^{13}C NMR, and ^{19}F NMR spectra for the new ionic liquid $[NapmC_1][NTf_2]$. This material is available free of charge via the Internet at http://pubs.acs.org.

■ AUTHOR INFORMATION

Corresponding Authors

*E-mail: sindee.simon@ttu.edu.
*E-mail: edward.quitevis@ttu.edu.

Funding

This research was supported by the Texas Tech Horn Professorship and Whitacre Department Chair Fund (SLS) and by National Science Foundation under Grant CHE-1153077 (ELQ). We thank the National Science Foundation for funding the purchase of the NMR instrumentation (CHE-1048553) used in this project.

Notes

The authors declare no competing financial interest.

REFERENCES

(1) Freemantle, M. Designer Solvents. *Chem. Eng. News* **1998**, *76*, 32−37.
(2) Welton, T. Room-Temperature Ionic Liquids. Solvents for Synthesis and Catalysis. *Chem. Rev.* **1999**, *99*, 2071−2083.
(3) Zhou, F.; Liang, Y. M.; Liu, W. M. Ionic Liquid Lubricants: Designed Chemistry for Engineering Applications. *Chem. Soc. Rev.* **2009**, *38*, 2590−2599.
(4) Van Valkenburg, M. E.; Vaughn, R. L.; Williams, M.; Wilkes, J. S. Thermochemistry of Ionic Liquid Heat-Transfer Fluids. *Thermochim. Acta* **2005**, *425*, 181−188.
(5) Galinski, M.; Lewandowski, A.; Stepniak, I. Ionic Liquids as Electrolytes. *Electrochim. Acta* **2006**, *51*, 5567−5580.
(6) Blanchard, L. A.; Hancu, D.; Beckman, E. J.; Brennecke, J. F. Green Processing Using Ionic Liquids and CO_2. *Nature* **1999**, *399*, 28−29.
(7) Han, X.; Armstrong, D. W. Ionic Liquids in Separations. *Acc. Chem. Res.* **2007**, *40*, 1079−1086.
(8) Fredlake, C. P.; Crosthwaite, J. M.; Hert, D. G.; Aki, S. N. V. K.; Brennecke, J. F. Thermophysical Properties of Imidazolium-Based Ionic Liquids. *J. Chem. Eng. Data* **2004**, *49*, 954−964.
(9) Zheng, W.; Mohammed, A.; Hines, L. G.; Xiao, D.; Martinez, O. J.; Bartsch, R. A.; Simon, S. L.; Russina, O.; Triolo, A.; Quitevis, E. L. Effect of Cation Symmetry on the Morphology and Physicochemical Properties of Imidazolium Ionic Liquids. *J. Phys. Chem. B* **2011**, *115*, 6572−6584.
(10) Dzyuba, S. V.; Bartsch, R. A. Influence of Structural Variations in 1-Alkyl(aralkyl)-3-Methylimidazolium Hexafluorophosphates and Bis(trifluoromethylsulfonyl)imides on Physical Properties of the Ionic Liquids. *ChemPhysChem* **2002**, *3*, 161−166.
(11) Huddleston, J. G.; Visser, A. E.; Reichert, W. M.; Willauer, H. D.; Broker, G. A.; Rogers, R. D. Characterization and Comparison of Hydrophilic and Hydrophobic Room Temperature Ionic Liquids Incorporating the Imidazolium Cation. *Green Chem.* **2001**, *3*, 156−164.
(12) Tokuda, H.; Hayamizu, K.; Ishii, K.; Susan, M. A. B. H.; Watanabe, M. Physicochemical Properties and Structures of Room Temperature Ionic Liquids. 2. Variation of Alkyl Chain Length in Imidazolium Cation. *J. Phys. Chem. B* **2005**, *109*, 6103−6110.
(13) Crosthwaite, J. M.; Muldoon, M. J.; Dixon, J. K.; Anderson, J. L.; Brennecke, J. F. Phase Transition and Decomposition Temperatures, Heat Capacities and Viscosities of Pyridinium Ionic Liquids. *J. Chem. Thermodyn.* **2005**, *37*, 559−568.
(14) Mandai, T.; Masu, H.; Imanari, M.; Nishikawa, K. Comparison between Cycloalkyl- and *n*-Alkyl-Substituted Imidazolium-Based Ionic Liquids in Physicochemical Properties and Reorientational Dynamics. *J. Phys. Chem. B* **2012**, *116*, 2059−2064.
(15) Mandai, T.; Matsumura, A.; Imanari, M.; Nishikawa, K. Effects of Cyclic-Hydrocarbon Substituents and Linker Length on Physicochemical Properties and Reorientational Dynamics of Imidazolium-Based Ionic Liquids. *J. Phys. Chem. B* **2012**, *116*, 2090−2095.
(16) Kulkarni, P. S.; Branco, L. C.; Crespo, J. G.; Nunes, M. C.; Raymundo, A.; Afonso, C. A. M. Comparison of Physicochemical Properties of New Ionic Liquids Based on Imidazolium, Quaternary Ammonium, and Guanidinium Cations. *Chem.—Eur. J.* **2007**, *13*, 8478−8488.
(17) Erdmenger, T.; Vitz, J.; Wiesbrock, F.; Schubert, U. S. Influence of Different Branched Alkyl Side Chains on the Properties of Imidazolium-Based Ionic Liquids. *J. Mater. Chem.* **2008**, *18*, 5267−5273.
(18) Deive, F. J.; Rivas, M. A.; Rodriguez, A. Thermophysical Properties of Two Ionic Liquids Based on Benzyl Imidazolium Cation. *J. Chem. Thermodyn.* **2011**, *43*, 487−491.
(19) Xia, Y.; Yao, M.; Liang, Y.; Zhou, F. *Process for Preparation of Naphthyl Containing Functionalized Ionic Liquids*. Patent CN102101842A, June 22, 2011.
(20) Badrinarayanan, P.; Zheng, W.; Li, Q. X.; Simon, S. L. The Glass Transition Temperature versus the Fictive Temperature. *J. Non-Cryst. Solids* **2007**, *353*, 2603−2612.
(21) Moynihan, C. T.; Easteal, A. J.; De Bolt, M. A.; Tucker, J. Dependence of the Fictive Temperature of Glass on Cooling Rate. *J. Am. Ceram. Soc.* **1976**, *59*, 12−16.
(22) Ye, C. F.; Shreeve, J. M. Rapid and Accurate Estimation of Densities of Room-Temperature Ionic Liquids and Salts. *J. Phys. Chem. A* **2007**, *111*, 1456−1461.
(23) Jenkins, H. D. B.; Roobottom, H. K.; Passmore, J.; Glasser, L. Relationships among Ionic Lattice Energies, Molecular (Formula Unit) Volumes, and Thermochemical Radii. *Inorg. Chem.* **1999**, *38*, 3609−3620.
(24) Traube, J. Ueber das Molekularvolumen. *Ber. Dtsch. Chem. Ges.* **1895**, *28*, 2722−2728.
(25) Kurtz, S. S.; Lipkin, M. R. Molecular Volume of Saturated Hydrocarbons. *Ind. Eng. Chem.* **1941**, *33*, 779−786.
(26) Davis, H. G.; Gottlieb, S. Density and Refractive Index of Multiring Aromatic Compounds in the Liquid State. *Fuel* **1963**, *42*, 37−54.
(27) Boyer, R. F. The Relation of Transition Temperatures to Chemical Structure in High Polymers. *Rubber Chem. Technol.* **1963**, *36*, 1303−1421.
(28) Cowie, J. M. G. *Polymers: Chemistry and Physics of Modern Materials*. 2nd ed.; CRC Press: Boca Raton, FL, 1991.
(29) Schmelzer, J. W. P.; Gutzow, I. S.; Mazurin, O. V.; Todorova, S. V.; Petroff, B. B.; Priven, A. I. *Glasses and the Glass Transition*; Wiley-VCH Verlag: Weinheim, Germany, 2011.
(30) Xu, W.; Wang, L. M.; Nieman, R. A.; Angell, C. A. Ionic Liquids of Chelated Orthoborates as Model Ionic Glassformers. *J. Phys. Chem. B* **2003**, *107*, 11749−11756.
(31) Fox, D. M.; Awad, W. H.; Gilman, J. W.; Maupin, P. H.; De Long, H. C.; Trulove, P. C. Flammability, Thermal Stability, and Phase Change Characteristics of Several Trialkylimidazolium Salts. *Green Chem.* **2003**, *5*, 724−727.
(32) Kosmulski, M.; Gustafsson, J.; Rosenholm, J. B. Thermal Stability of Low Temperature Ionic Liquids Revisited. *Thermochim. Acta* **2004**, *412*, 47−53.
(33) Baranyai, K. J.; Deacon, G. B.; MacFarlane, D. R.; Pringle, J. M.; Scott, J. L. Thermal Degradation of Ionic Liquids at Elevated Temperatures. *Aust. J. Chem.* **2004**, *57*, 145−147.
(34) Del Sesto, R. E.; McCleskey, T. M.; Macomber, C.; Ott, K. C.; Koppisch, A. T.; Baker, G. A.; Burrell, A. K. Limited Thermal Stability of Imidazolium and Pyrrolidinium Ionic Liquids. *Thermochim. Acta* **2009**, *491*, 118−120.
(35) Maton, C.; De Vos, N.; Stevens, C. V. Ionic Liquid Thermal Stabilities: Decomposition Mechanisms and Analysis Tools. *Chem. Soc. Rev.* **2013**, *42*, 5963−5977.
(36) Salgado, J.; Villanueva, M.; Parajo, J. J.; Fernandez, J. Long-Term Thermal Stability of Five Imidazolium Ionic Liquids. *J. Chem. Thermodyn.* **2013**, *65*, 184−190.
(37) Simon, S. L.; Gillham, J. K. Cure Kinetics of a Thermosetting Liquid Dicyanate Ester Monomer/High-T_g Polycyanurate Material. *J. Appl. Polym. Sci.* **1993**, *47*, 461−485.
(38) Chan, B. K. M.; Chang, N.; Grimmett, M. R. The Synthesis and Thermolysis of Imidazole Quaternary Salts. *Aust. J. Chem.* **1977**, *30*, 2005−2013.